

An analytical model for noise radiated from axial vibration of a simplified pressure hull of an underwater vehicle

Marshall V. Hall¹

¹Marshall Hall Acoustics
Kingsgrove NSW 2208, Australia
Email: marshallhall@optushome.com.au

Abstract

An analytical model is presented for the hull vibration and sound pressure radiated when a large empty cylindrical hull submerged in water is excited by an axial thrust along a central propeller shaft. The model, which is based on the Donnell-Mushtari coupled equations of motion for axial and radial vibration of a cylindrical shell, yields frequency-dependent phase velocity and attenuation of those vibrations. The amplitudes of the vibrations that travel along a hull and reflected by both ends are described in terms of the incident thrust. A solution is obtained for the consequent radiated sound pressure. Both unstiffened and stiffened shells are considered, in which the analytical model for the stiffened shell is based on a smeared approach. Results from the analytical model presented here are compared with the analytical results from literature. The main contribution of this work is to consider phase velocities that vary with frequency and their effect on the radiated sound pressure.

1. Introduction

An underwater vehicle (“submersible”) is simplified to a thin cylindrical shell with a thin circular plate fixed to each end. The effect of the thrust of the propeller is represented by a harmonic (single-frequency continuous wave) axial thrust acting on one end of the shell, referred to as the stern. Axial and radial displacement waves travel along the shell, reach the far end (the bow) and are reflected backwards. The backward travelling waves are in turn reflected forward by the stern, and this process continues indefinitely, albeit with diminishing amplitude.

Due to the radial displacement, sound waves radiate into the surrounding water, and their pressure may be predicted. The purpose of developing a simple model of such radiated sound is to examine the physics of the sound generation. The practical aim of predicting the pressure, even approximately, that would radiate from a real submersible is not addressed. Nevertheless, an understanding of this physics is a necessary first step towards the development of a realistic model.

There have been many papers published on this topic, several of which came from the School of Mechanical and Manufacturing Engineering at the University of NSW. Of those papers, [1] and [2] are referred to heavily in the present paper. The main difference between the present analysis and earlier papers is that this paper determines the complex dispersive phase velocity of the displacement waves, and goes on to estimate the consequent radiated sound pressure.

The present paper contains few equations; those omitted are available in [3] for the cylindrical shell, and in [4] and [5] for the plates.

2. The cylindrical shell

The three cylindrical coordinates used are the axis (x), longitude (θ) and radius (r). The corresponding components of shell displacement are u , v and w , as shown in Figure 1.

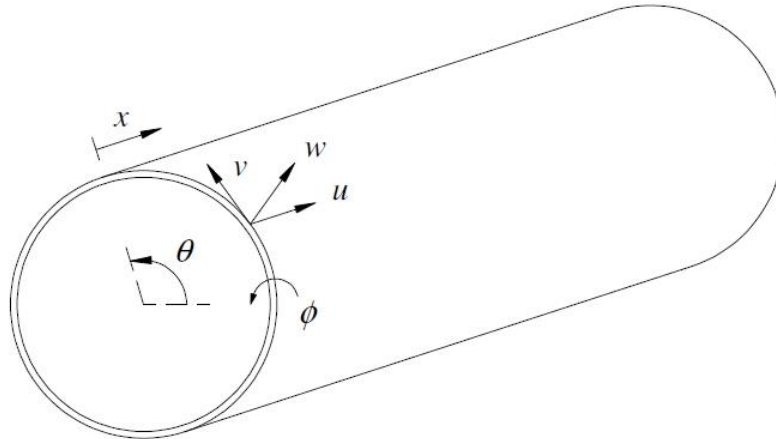


Figure 1. Coordinates and displacements (u,v,w) for a thin cylindrical shell. The radial coordinate is not depicted. The angle ϕ denotes the (small) slope of the shell wall in the (negative) axial direction.

2.1 Assumptions

The assumptions made for an unadorned cylindrical shell are standard, but are listed here for convenience. Discussions on these may be found in [6], [7] and [8]. A recent summary is provided by [3].

- The shell's thickness (h) is small ($< 10\%$) in relation to its radius (a).
- Radial displacements (w) are small in relation to the shell thickness.
- The transverse normal stress acting on planes parallel to the shell middle surface is negligible.
- Portions of the shell normal to the reference surface of the shell remain normal to it, and undergo no change in length during deformation.
- The radius and wall thickness are constant.
- The wall thickness is small in relation to the wavelength of the elastic wave within it.
- The shell does not twist, and the displacements are independent of longitudinal angle (θ) around the shell axis.
- Bending of the shell (dw/dx) is small.
- The shell is immersed in only one medium, which is a non-viscous liquid of infinite extent.
- The medium inside the shell is either a vacuum or a light gas.
- Structural damping in the shell is characterized by a loss factor ($1/Q$).

The main consequences of these assumptions are that (1) the axial and radial displacements are independent of radius and longitude, and are thus functions of axial distance only, and (2) the longitudinal displacement (v) is zero.

In addition to the unadorned shell, the effects of “added mass” and stiffening were examined by [2]. “Added mass” refers to the mass of the items that are usually found in a submersible other than its shell. One practical purpose in adding mass is to increase the average density of the submersible to be in the neighbourhood of that of the surrounding medium. At low frequencies, the effect of added mass on shell vibration is approximated by considering the mass to be distributed evenly over the shell surface. It increases the shell density and thus lowers the shell's plate velocity (q_p).

“Stiffening” refers here to reinforcement of the cylindrical shell using internal uniformly spaced ring stiffeners with rectangular cross section. At low frequencies, the effect of these rings on shell vibration is approximated by averaging their properties over the surface of the cylindrical shell (the shell wall is made commensurately thicker).

The adjustments that need to be made to some terms in the equations of motion, in order to allow for added mass and stiffening, were listed in [2].

2.2 Equations of motion

Since the thrust is steady-state and harmonic, each variable varies with time simply as $\exp(i\omega t)$. The displacements are functions of distance only, and are written as $u(x)$ and $w(x)$.

The assumed equations of motion are in accord with the ‘‘Donnell-Mushtari’’ operator as catalogued by [9], except that the term proportional to d^4w/dx^4 is neglected. This term is proportional to the square of the shell thickness and the fourth power of frequency, and it follows from the analysis in a comparable study [3] that it may be neglected over the low-frequency band to be examined in the present paper. Given that $v(x) = 0$ and there is no dependence on longitude (the ‘‘n = 0’’ longitude mode), the equations of motion simplify to two coupled equations in $u(x)$ and $w(x)$, in which the coupling terms can be eliminated with a little algebra. One of them reduces to [3]:

$$w(x) = C \, du(x)/dx \quad (1)$$

in which C depends on frequency and the shell’s physical properties, but is independent of x .

The equations of motion for the cylindrical shell are solved in two stages. In the first stage, the ends are neglected (the shell length is assumed to be infinite). In this stage, it is found that $u(x)$ satisfies a Helmholtz equation. The phase velocity of $u(x)$ will be denoted by $V_P(\omega)$.

2.3 Specifications of the cases considered

Spectra of phase velocity (V_P) have been computed for the single case considered in [1] and also for the two cases considered by [2]. The first case (to be denoted by ZK00) has no added mass or stiffening. The second case (m0) has added mass with no stiffening, and the third case (ms) has both added mass and stiffening. The specifications that are common to all three cases are summarised in Table 1. It can be seen from the Young modulus and density that the shell is assumed to be made of steel.

Table 1. Physical properties of the cylindrical shell common to the three cases.

PARAMETER	VALUE
Radius, a	3.25 m
Wall thickness, h	0.04 m
Young modulus, Y	210 GPa
Density, ρ_s	7800 kg/m ³
Bar velocity, $q = \sqrt{Y/\rho_s}$	5189 m/s
Plate velocity, $q_p = q/\sqrt{1 - \nu^2}$	5439 m/s
Poisson ratio, ν	0.3
Loss factor, $1/Q$	0.02 (corresponds to axial damping rate of 0.55 dB per wavelength)

For added mass, the density used by [2] was 1500 kg /m² over the shell surface area.

The internal stiffeners modelled by [2] had a rectangular cross-section of 0.08 m \times 0.15 m and were spaced 0.5 m apart.

2.4 Results for Phase velocity of axial vibration

The variable V_P is complex. The spectra of $\text{Real}\{V_P\}$ that resulted for the three cases are shown in Figure 2. Since the frequency bands presented by [1] and [2] had maximum frequencies of up to 100 Hz, a maximum frequency of 100 Hz is used here. It can be seen from Figure 2 that the added mass reduces V_P from around 5200 m/s to around 2100 m/s, and the stiffening decreases it slightly further.

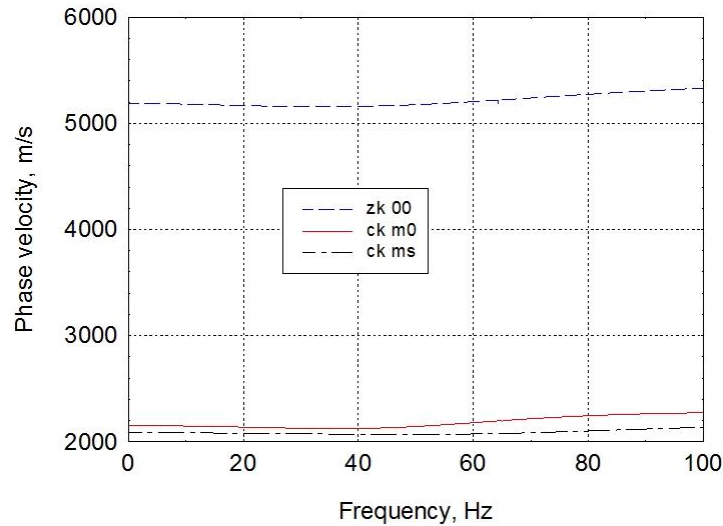


Figure 2. Spectra of axial phase velocity for the three cases examined. In the legend, ‘zk 00’ denotes the [1] case which had no added mass or stiffening, ‘ck m0’ denotes the [2] case with no stiffening, and ‘ck ms’ denotes the [2] case with stiffening.

2.5 Damping of axial vibration

The imaginary part of V_P corresponds to an axial damping coefficient. For each of the three cases, the damping in decibels per wavelength is shown in Figure 3. At each frequency, the wavelength was obtained by dividing $\text{Real}\{V_P\}$ by frequency. As frequency approaches zero, the damping approaches $0.55 \text{ dB}/\lambda$, the intrinsic loss factor in the steel shell. The damping of the waves in the shell is due to the transfer of energy from the shell into the surrounding medium.

It can be seen that stiffening reduces the damping, while added mass increases it. Taking case m0 for example, the maximum damping of $3.6 \text{ dB}/\lambda$ occurs at around 65 Hz, where V_P is around 2200 m/s. An axial wave will attenuate by 3.6 dB after travelling a distance of one wavelength (34 m). Successive reflections in a shell of length 45 m (the length used in [1] and [2]) will thus become insignificant after a small number of traverses along the submersible, regardless of the reflectivity at the ends.

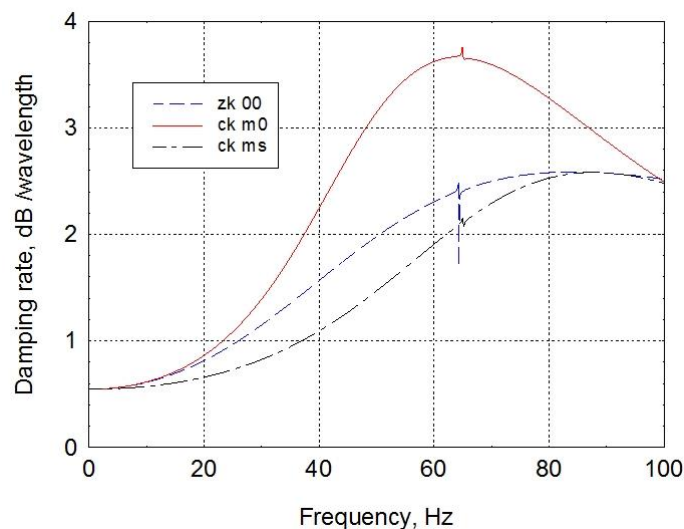


Figure 3. Spectra of axial damping coefficient for the three cases examined. The symbols in the legend have the same meaning as in Figure 2.

3. The end plates

The submersible has a solid circular plate attached to each end of the cylindrical shell. The coordinates and displacements of such a plate are shown in Figure 4. A cylindrical shell attached to an end plate cannot be treated as a free shell; boundary conditions are needed to solve for the displacement distribution. There are no longer any pure cylindrical shell modes - only plate / shell coupled modes. For example, the slopes of the plate and shell should be equal as the edge of each plate is rigidly connected to the end of the shell (Colin Hansen, personal communication).

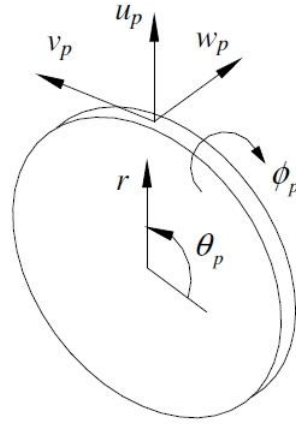


Figure 4. Polar coordinates and displacements for a thin end plate. The axial displacement w_p is transverse (perpendicular) to the plate. The angle ϕ_p denotes the (small) slope of the plate in the axial direction.

The interaction between the shell and plate at their junction, insofar as the shell displacements u and w are concerned, is assumed to be independent of the radial plate displacement (u_p). This follows from considering the shell's axial displacement to be the driver of radial displacement. These displacements are not independent, as can be seen from Eq. (1).

The reflectivity of the radial displacement wave at each end is not used in the model, whereas the reflectivity of the axial displacement wave is used. Although the shell's and plates' radial displacements will have to match at each junction, this is neglected in the model, since at all other positions radial displacement will be determined by Eq. (1).

The reflectivity of the axial displacement wave at each shell end is the same, and may be computed by taking into account the boundary conditions that arise from the shell's attachment to end plates.

The consequence of the above assumptions is that the boundary conditions at the junction are independent of u_p . It is therefore sufficient to examine the equation of motion for w_p , which is a fourth-order differential equation [5]. For a solid circular plate (as distinct from an annulus) the solution for the $n = 0$ longitude mode may be written as the sum of a zero-order Bessel and modified Bessel functions. Their frequency-dependent coefficients, to be denoted by A and B , are to be determined. Although eight boundary conditions at a junction were listed by [5], only three boundary conditions are required under the assumptions made here:

- (i) displacements: axial displacement at either end of the shell matches the transverse displacement at the plate edge.
- (ii) slopes: the slope of the shell wall relative to the axis, $dw(0)/dx$, matches the slope of the plate at its edge relative to the radial plane, $dw_p(a)/dr$. This follows from the shell edge being rigidly fixed to the plate (at its edge).
- (iii) forces: axial force in the shell matches the transverse force at the plate edge. Expressions for these forces were obtained from [10] and [11] respectively.

For a shell of finite length (L), the solution to the Helmholtz equation for $u(x)$ is the infinite sum of travelling waves travelling forward and astern, successively reflected by the end junctions. The (frequency-dependent) reflectivity (R_L) together with the plate coefficients A and B are the three

unknowns that may be obtained by solving the three linear equations that result from the three boundary conditions.

4. Results for the end reflectivity

In computing the end reflectivity, it is noted that according to [1] and [2] the plates have the same physical properties as the cylindrical shell, including its thickness. The spectrum of the complex reflectivity obtained for the ZK00 case from [1] is shown in Figure 5. The reflectivity is approximately +1 at most frequencies, with exceptions occurring at frequencies of 10, 38 and 84 Hz. These correspond closely (within 1 Hz) to the first three harmonic frequencies of vibration in the end plates observed by [1].

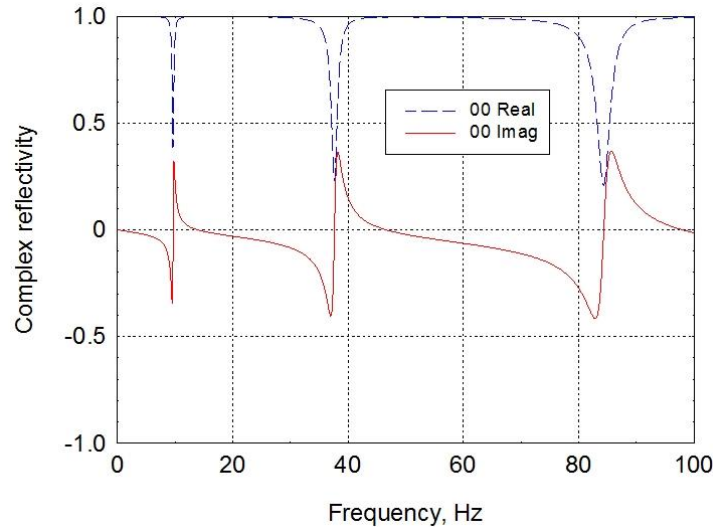


Figure 5. Complex reflectivity of shell axial displacement waves incident at a shell end, for the ZK00 case from [1].

The spectrum of the complex reflectivity obtained for the ms case from [2] is shown in Figure 6 (that for the m0 case is similar). This spectrum differs from the ZK00 case in that (i) the departures below +1 occur over wider frequency bands around the plate's harmonic frequencies, (ii) the real part extends to negative values at those frequencies, and (iii) the imaginary parts are greater.

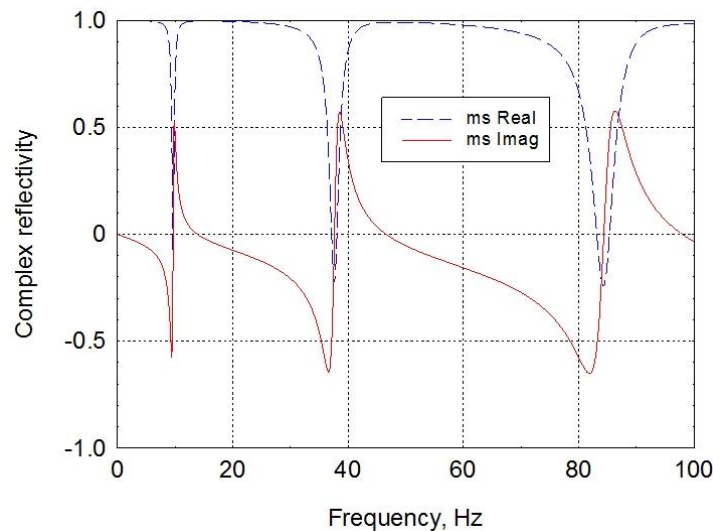


Figure 6. Complex reflectivity of shell axial displacement waves incident at a shell end, for the ms case from [2].

5. Results for axial and radial displacements

The axial thrust considered by [1] was harmonic, had a magnitude of 1 N and was applied to a small area at the centre of the stern circular plate ($x = 0, r = 0$). For this application the plate equation of motion is an inhomogeneous differential equation (it has an external forcing function), and this scenario is beyond the scope of the present paper. The main purpose in addressing this case was to show that at low frequency V_P is comparable with the shell bar velocity.

The axial thrust considered by [2] was harmonic, had a magnitude of 1 N and was applied to a small area on the stern edge of the cylindrical shell ($x = 0, r = a, \theta = 0$). This thrust would stimulate many longitude modes (characterised by a dependence of $\cos n\theta$), but here the excitation of only the $n = 0$ mode is considered. By expanding the angle-dependence of the incident stress as a series of terms in $\cos n\theta$, and integrating over a full longitudinal rotation, it is found that the zero-order component of stress is simply the thrust divided by the area of the annular edge ($2\pi ah$). The incident stress that stimulates the $n = 0$ longitude mode is therefore equivalent to the full thrust acting over the annular edge, notwithstanding that it will also generate angle-dependent modes (presumably they sum to zero). Spectra of axial displacement for the $n = 0$ longitude mode obtained for the m_0 (not stiffened) and m_s (stiffened) cases are shown in Figure 7. An axis position of $x = 9.27$ m was chosen, in order to accord with [2]. On comparing this Figure 7 with the corresponding figure in [2] it can be seen that there is excellent agreement for both cases at frequencies less than 40 Hz, except that the present figure displays the 10-Hz plate resonance more strongly. At higher frequencies the agreement is moderately good; the maximum and minimum near 70 Hz are smooth here but sharp in [2]. In making this comparison it is necessary to take into account that there are typographical errors in the ordinate labels in [2] that report decibel values; the numbers displayed are half the correct values (Nicole Kessissoglou, personal communication).

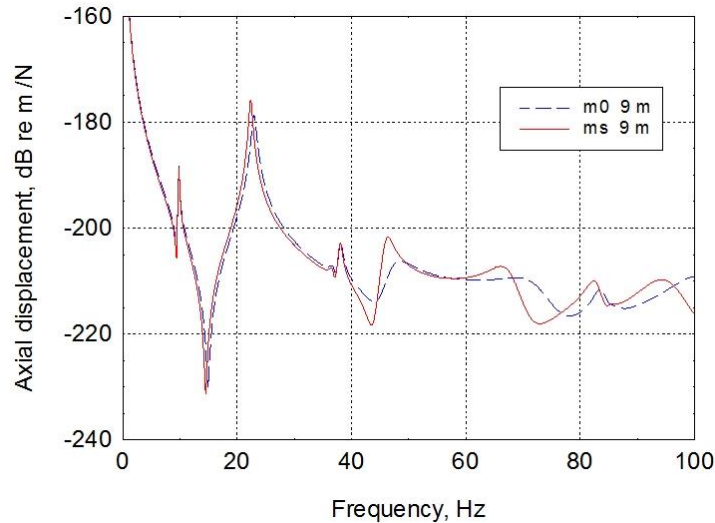


Figure 7. Spectra of axial displacement for the $n = 0$ longitude mode at $x = 9.27$ m, obtained for the m_0 (not stiffened) and m_s (stiffened) cases.

Spectra of radial displacement obtained for the m_0 and m_s cases from [2] are shown in Figure 8. On comparing Figure 8 with the corresponding figure in [2] it can be seen that there is excellent agreement for both cases at frequencies less than 40 Hz, except that the present figure displays the plate's first harmonic frequency at 10 Hz whereas there is no sign of it in [2]. At higher frequencies the agreement is not as good, the main difference being that the minimum near 60 Hz and the maximum near 70 Hz are smooth here but sharp in [2].

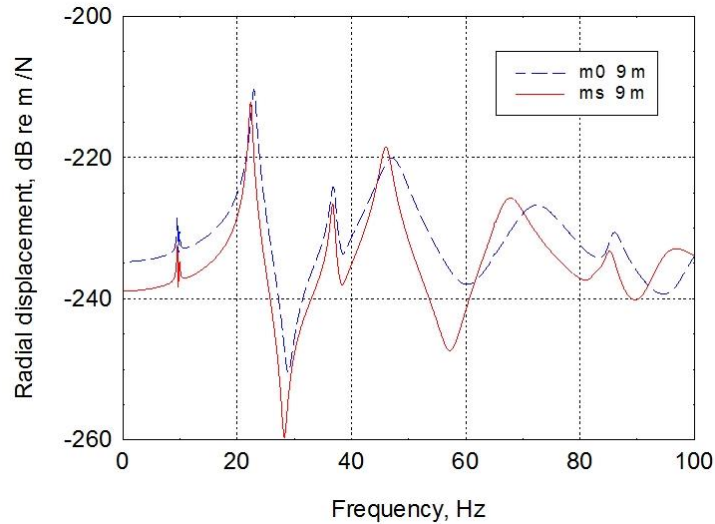


Figure 8. Spectra of radial displacement for the $n = 0$ longitude mode at $x = 9.27$ m, obtained for the m_0 (not stiffened) and m_s (stiffened) cases.

On comparing Figures 7 and 8 together with the corresponding figures in [2] (which extended to only 80 Hz) it can be seen that the plate's first harmonic frequencies are consistent, while the plate's second harmonic occurs at 38 and 37 Hz here (for cases m_0 and m_s respectively), compared with 34 Hz in [2]. The plate's third harmonics appear to occur here at between 82 and 85 Hz. For the cylindrical shell, the first harmonics occur at 23 and 22 Hz for the two cases, the second harmonics occur at 47 and 46 Hz, and the third harmonics occur at 72 and 68 Hz. In each case the shell's harmonic frequencies obtained here are consistent with [2] to within 1 Hz.

6. Radiated sound

The sound pressure radiated by the radial motion of the cylindrical shell has been calculated using Junger and Feit's "Transform formulation of the pressure field of cylindrical radiators" [12]. The far-field pressure is given by their "stationary phase approximation to the far-field of cylindrical radiators". A slant range of 1000 m was selected, consistent with [2] (the word 'slant' is included to emphasise that the range is the length of the vector from the submersible to the receiving point, as distinct from the component in the radial plane which will vary with colatitude). The resulting spectra of sound pressure radiated by the cylindrical shell on a colatitude of 90° (abeam of the submersible) for the m_0 and m_s cases are shown in Figure 9.

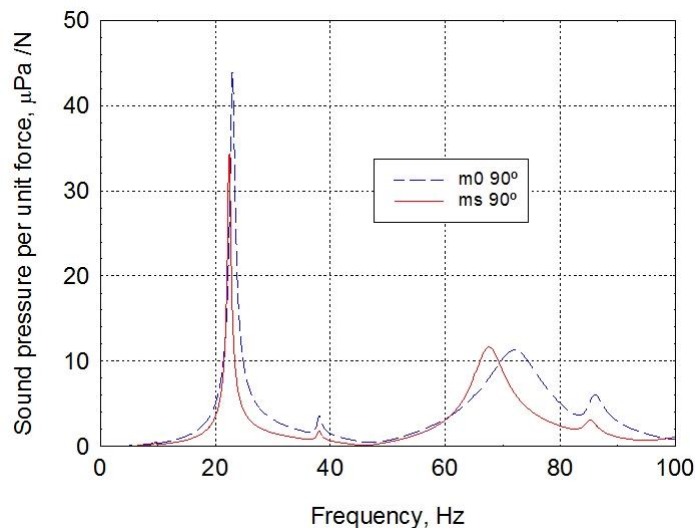


Figure 9. Spectra of sound pressure radiated by cylindrical shell at range 1000 m on a colatitude of 90° , for the m_0 and m_s cases. Longitude mode $n = 0$.

The effects of the plate's second and third harmonics are evident in Figure 9, as are the shell's first and third harmonics. The shell's second harmonic is very small at this (abeam) colatitude, due to the two halves of the shell vibrating out of phase at this frequency.

Sound pressures radiated by the cylindrical shell at range 1000 m have been computed at the shell's first three harmonic frequencies. Their magnitudes are shown in Figure 10 as functions of colatitude for the m0 case. The first harmonic (23 Hz) varies slowly and has a maximum of 44 μPa (33 dB re μPa) at 90°. The second harmonic (47 Hz) has a null at 90° and smooth peaks at 50° and 125°. The real part of the pressure changes in phase from positive to negative at 90°. The magnitude of the third harmonic (72 Hz) has two sharp minima at 77° and 103°. The former is not a null in the magnitude; the pressure's real part is zero but in this case its imaginary part is significant. The pressure's real part has two smooth positive peaks at 48° and 128°, and a negative peak at 90°.

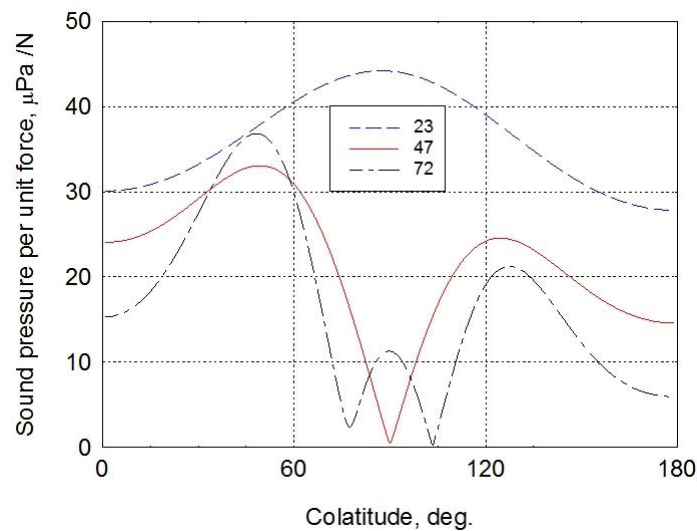


Figure 10. Magnitude of sound pressure radiated by cylindrical shell at range 1000 m as a function of colatitude, at the shell's first three harmonic frequencies for the m0 case (23 Hz, 47 Hz and 72 Hz). Longitude mode $n = 0$.

7. Remarks and conclusions

An independent model has been developed for the noise radiated from a submersible that can be modelled as a thin cylindrical shell capped rigidly with two thin end plates. The axial displacement wave has a dispersive phase velocity that possesses a significant imaginary part over substantial frequency bands. As a consequence, the amplitude of the axial displacement (and its related radial displacement) decays with distance travelled along the shell axis. This decay is a measure of the transfer of energy from within the shell to the external medium.

Comparison of results from the analytical model presented here with results from the literature (that assumed phase velocity to be non-dispersive) shows that the harmonic frequencies match to within 1 Hz for the shell and to within 11% for the plate. The differences between the new and existing displacement spectra are negligible at low frequencies but become noticeable at higher frequency. This effect may be attributed to the dispersion in phase velocity.

As a consequence of differences in the data presented, it is difficult to make a precise comparison of the sound pressure levels displayed in this paper with those presented by [2]. At any frequency in a sound pressure spectrum, [2] reported the maximum pressure over a complete rotation of colatitude, rather than on a fixed colatitude as presented here. As a generalisation, the pressures presented here appear to be approximately one half of their counterparts in [2]. This reduction may be attributable, at least in part, to the damping of the shell displacement waves.

It is of interest that the magnitude of the considered thrust is very small; a thrust of 1 N from a 1-MW engine for example would yield a speed of 1 μ /s. The resulting displacements are also very small

(-200 dB re m is equivalent to 1 Angstrom, the radius of an atom of iron). To produce a practical speed of 10 m/s with the same engine would require a thrust of 10 MN, an increase of 140 dB. The maximum sound pressure of the first harmonic for a practical scenario would therefore increase from 33 dB re μPa to 173 dB re μPa .

Acknowledgements

The AAS NSW Division provided a significant financial contribution in order to support my attendance at this conference.

Nicole Kessissoglou has been a helpful source of information on similar work done by her group in the School of Mechanical and Manufacturing Engineering at the University of New South Wales. Figures 1 and 4 were copied with permission from documents produced by that group.

Colin Hansen provided the explanation of the boundary conditions at the junction between the cylindrical shell and each plate.

References

- [1] Zhang C and Kessissoglou N, “Effect of excitation loads on the low frequency structural responses of a submerged hull”, *Proceedings of Acoustics 2012 – Fremantle*, pp 163 – 167 (2012).
- [2] Caresta M and Kessissoglou NJ, “Structural and acoustic responses of a fluid-loaded cylindrical hull with structural discontinuities”, *Applied Acoustics*, **70**, 954 – 963. (2009)
- [3] Hall MV, “An analytical model for the underwater sound pressure waveforms radiated when an offshore pile is driven”, *Journal of the Acoustical Society of America* **138**, 795 – 806 (2015).
- [4] Love AEH, *A Treatise on the Mathematical Theory of Elasticity*, Fourth edition Dover Publications, New York, 1944 (p. 496).
- [5] Tso YK and Hansen CH, “Wave propagation through cylinder/plate junctions”, *Journal of Sound and Vibration* **186**, 447-461 (1995).
- [6] Reference [4], pp. 515-537.
- [7] Junger MC and Feit D, *Sound, Structures, and Their Interaction*, Acoustical Society of America, New York, 1993 (p. 216).
- [8] Kraus H, *Thin elastic shells*, John Wiley & Sons, Inc., New York, 1967.
- [9] Leissa AW, *Vibration of shells*, American Institute of Physics, Woodbury, New York, 1993 (page 32).
- [10] Reference [4], page 488.
- [11] Reference [9], page 14.
- [12] Reference [7], pages 173-176